

# Ni-W Alloy Coating as an Efficient Electrocatalyst for the Hydrogen Evolution Reaction: Effect of Electroplating Current Density on Morphology and Electrocatalytic Properties

Mohammad Derakhshani<sup>1</sup>, Saeed Rastegari<sup>1,\*</sup>, Ali Ghaffarinejad<sup>2</sup>

\* rastegari@iust.ac.ir

<sup>1</sup> School of Metallurgy and Materials Engineering, Iran University of Science & Technology, Tehran, Iran

<sup>2</sup> Electroanalytical Chemistry Research Center, Iran University of Science and Technology, Tehran, Iran

Received: January 2024

Revised: April 2024

Accepted: May 2024

DOI: 10.22068/ijmse.3482

**Abstract:** This research synthesized a nickel-tungsten coating as a catalyst for hydrogen evolution reaction (HER) with different current densities and assessed the resulting electrocatalytic properties and morphology. Linear sweep voltammetry (LSV), electrochemical impedance spectroscopy (EIS), and chronoamperometry in 1 M NaOH were used to evaluate the electrocatalytic activity for HER. A columnar morphology was observed by increasing the current density of electrodeposition up to 500 mA/cm<sup>2</sup>. The cyclic voltammetry test (CV) revealed that when the plating current density increases, Cdl increases from 248 to 1310 μF/cm<sup>2</sup> and the active surface area increases 5 times. The results showed that by modifying the coating morphology, the current density of the hydrogen evolution increased up to two times.

**Keywords:** Electroplating, Coating, Hydrogen evolution reaction, Porous materials, Electrocatalyst.

## 1. INTRODUCTION

Two main problems that will affect human life in the future are the pollution of the environment and the depletion of fossil fuels (1-3). Therefore, developing and applying renewable and clean energy sources is a very important necessity that has received much attention (4). One source of clean, unlimited, and readily available energy is hydrogen, which has a higher energy density than hydrocarbon fuels. One of the methods of hydrogen production is the use of hydrocarbon resources, which also has the two primary issues mentioned above (5-7). Electrolyzing water to obtain pure hydrogen is another method that many researchers are currently trying to expand. Most of the hydrogen on Earth is found in water, which makes up more than two-thirds of the planet (8, 9). Thus, electrolysis is an easy and safe method with an infinite source, and the need to expand its use is well understood (10, 11).

Platinum exhibits high electrocatalytic activity due to its high exchange current density and low overvoltage. On the other hand, the high cost and rarity of this noble metal increase the cost and restrict its applications. For this reason, many attempts have been made to find a suitable alternative to platinum with optimal electrocatalytic activity as well as low cost (12-14). Transition metals, especially nickel, are one

of the most promising alternatives to platinum with high electrocatalytic properties. Many efforts have been made to improve the electrocatalytic properties of nickel by alloying and fabricating nickel-based composites, with acceptable and promising results (15-20).

Combining metals on the left or right of a transition metal in the periodic table, i.e., the combination of metals with vacant or half-occupied d orbitals with metals whose d orbitals have electron pairs leads to a significant increase in the density of electron states and thus raises the electrocatalytic property for the hydrogen evolution reaction (HER). Alloying nickel ([Ar] 3d<sup>8</sup>4s<sup>2</sup>) with tungsten ([Xe] 4f<sup>14</sup>5d<sup>4</sup>6s<sup>2</sup>) yields satisfactory results (21). In this regard, researchers have achieved high catalytic activity by changing specific factors and studying the effects of these factors on the electrochemical behavior of the Ni-W coating (22-24). In the following sections, we study the effect of some of these factors. Jameei Rad et al. (25) synthesized a nickel-tungsten coating by electroplating on a copper cathode, and in the next stage, they created a more active surface and enhanced the surface roughness by etching the electrode surface, which ultimately increased the electrocatalytic property as well as HER. Moreover, the degree of wettability of the coating and its effect on hydrogen production have been examined and

reported.

Vernickaite et al. (6) investigated the effect of tungsten addition on nickel, iron, and cobalt and the alloying of these metals and reported that the nickel-tungsten alloy has the best electrocatalytic properties as well as the lowest activation energy to start HER. They also concluded that by increasing the amount of tungsten, nanostructured intermetallic compounds are formed, which have a positive effect on HER.

Allam et al. (21) worked on a Ni-W-Mo alloy and obtained coatings with different chemical compositions by changing the  $\text{Mo}_4^{2-}/\text{WO}_4^{2-}$  ratio in the plating bath. They reported that the electrocatalytic properties were enhanced compared with those of pure nickel due to the synergistic effect.

As mentioned in the literature, hydrogen evolution can be improved by strengthening the intrinsic electrocatalytic properties and increasing the active surface (26). This can be obtained by several methods, one of which is to change the surface morphology and the way the deposits grow during the electrodeposition process. Therefore, this research aimed to change the morphology of the nickel-tungsten alloy coating by using the columnar growth mechanism. To accomplish this purpose, high current density was used. In this paper, the morphological changes of the coating were investigated and the electrocatalytic properties of HER were analyzed using electrochemical impedance spectroscopy (EIS) and linear sweep voltammetry (LSV). The stability of the coating was also evaluated using the chronoamperometry test, and the results were reported.

## 2. EXPERIMENTAL PROCEDURES

St37 steel plates with a thickness of 2 mm were used as the substrates. They were cut into 5 cm × 3 cm pieces and ground using SiC papers with a grit size of up to grit 1000. The substrates were ultrasonically degreased by acetone for 15 min and then were activated in a solution containing 10 wt.% HCl. Activation was performed for 30 seconds at 25°C. Finally, they were washed with distilled water.

The composition of the bath used is presented in Table 1 (20, 27). Plating was performed at 60°C for 30 min. The pH of the solution was adjusted

to pH= 9 by the addition of ammonia and sulfuric acid. Pure nickel plates with dimensions of 7 cm × 4 cm were used as the anode. Electrodeposition was performed at average currents of 300, 400, and 500 mA/cm<sup>2</sup>. Plating was carried out in the pulsed mode with a working cycle of 70% and a frequency of 100 Hz. The distance between the anode and cathode was 3 cm and the stirring speed was 200 rpm.

**Table 1.** Composition of the Ni-W plating bath

NiSO <sub>4</sub> .7H <sub>2</sub> O	15.8 g/l
Na <sub>2</sub> WO <sub>4</sub> .2H <sub>2</sub> O	46.2 g/l
Na <sub>3</sub> C <sub>6</sub> H <sub>5</sub> .2H <sub>2</sub> O	147.1 g/l
NH <sub>4</sub> Cl	26.7 g/l
NaBr	15.4 g/l

The X-ray diffraction (XRD) analysis was used to detect the phase composition (DRON-8,  $K_{\alpha, \text{Cu}} = 1.54 \text{ \AA}$ ), field emission scanning electron microscopy (FESEM) was employed to examine the surface morphology, and energy dispersive spectroscopy (EDS) spectroscopy was used to determine the chemical composition of the coatings (TESCAN Company). LSV, EIS, and chronoamperometry were utilized to evaluate the electrocatalytic properties. Three electrode tests were performed with the platinum electrode as the counter electrode, the as-coated sample as the working electrode, and the calomel reference electrode in 1 M NaOH solution (28). EIS was performed in the range of 100 kHz to 10 mHz under a cathodic potential of -1.1 V and a sinusoidal signal amplitude of 10 mV. Chronoamperometry was also conducted at a cathodic voltage of -1.5 V and a time of 3 hours. Electrochemical analyses were carried out by the Autolab PGSTAT204 device.

## 3. RESULTS AND DISCUSSION

### 3.1. Morphology and Microstructure of the Coating

Figure 1 shows the morphology of the coating obtained using different current densities. As can be observed, coarse grains and dense cauliflower structures were formed at 300 mA/cm<sup>2</sup> (Fig. 1a). By raising the current density to 400 mA/cm<sup>2</sup> (Fig. 1b), the vertical growth rate exceeded the horizontal growth rate. For this reason, the hollow cylinders inside the coating found no chance of growth and joining each other. Figure 1d shows

an inside view of these cylinders. These cylinders expanded the surface area of the coating. By increasing the current density to 500 mA/cm<sup>2</sup> (Fig. 1c), the growth of the coating formed parallel columns that were placed next to each other and grew, and the horizontal growth of these columns was significantly reduced. In Fig. 1e, the growth front of one of these columns can be seen at a higher magnification, which has a sharp roughness at the nanometer scale. These are effective in increasing the surface area and surface roughness.

The XRD pattern of the coating electrodeposited with a current density of 500 mA/cm<sup>2</sup> is shown in Fig. 2a. Diffraction peaks of Ni (1 1 1) and Ni (2 0 0) are indicative of the nickel crystal in Fcc structure. The nickel peaks exhibit a certain deviation from those of pure nickel. This indicates that the nickel atoms are partially replaced with tungsten atoms and that the Ni-W solid solution is formed, which leads to the increase of the lattice parameter and the shift of the nickel peak to a lower angle. The results of the EDS mapping

analysis are displayed in Fig. 2c and 2d and prove the simultaneous and scattered presence of nickel and tungsten in the coating. The results of the EDS analysis revealed that the atomic percentages of tungsten and nickel were 10 and 90, respectively.

### 3.2. Investigation of Electrocatalytic Properties $\mu\text{m}$

#### 3.2.1. Results of LSV testing

Figure 3 shows the results of the LSV test investigating the electrocatalytic properties of the coatings. It is clear that with the rise in the current density, the occurrence of columnar growth in the coating, and the improvement in the catalyst properties, the potential to start HER shifted to more positive values. As a result, the catalyst required a lower amount of energy to start the reaction. In addition, at a certain overpotential, the amount of cathodic current density increased, which indicates a higher reaction rate. This improvement in the properties continued up to 500 mA/cm<sup>2</sup>.



**Fig. 1.** Surface morphology of the samples electrodeposited with different current density a- 300 mA/cm<sup>2</sup>, b- 400 mA/cm<sup>2</sup>, c- 500 mA/cm<sup>2</sup>, d- 400 mA/cm<sup>2</sup> with higher magnification, e - 500 mA/cm<sup>2</sup> with higher magnification.





**Fig. 2.** a) Results of XRD analysis, b) SEM image of the Ni-W sample, c) EDX map of Ni distribution, d) EDX map of W distribution of the coating electrodeposited with a current density of 500 mA/cm<sup>2</sup>.

In fact, in addition to the inherent nature of the electrode, increasing its active surface also played an important role in its catalytic activity, which is due to the rise in the electron transfer sites between hydrogen and the electrode surface. By expanding the active surface of electrodes, more sites became available for hydrogen ions and more ions were reacting at the same time.



**Fig. 3.** Results of LSV test on Ni-W coating electrodeposited with different current densities.

The results showed that both the cathodic current density of hydrogen evolution and the catalytic activity of the electrode were increased twofold.

### 3.2.2. EIS test

EIS tests were performed on the samples to further investigate the electronegativity properties, and the results of Nyquist diagrams can be observed in Fig. 4. In this experiment, the potential of the samples was in the negative cathodic range of 1 V concerning the calomel reference electrode to evaluate HER kinetics. The equivalent circuit is also shown in Fig. 4, which includes  $R_s$  (i.e., the solution resistance),  $R_p$  (the charge transfer resistance), and  $Q$  (the constant phase element). This experiment indicated that by increasing the electroplating current density, the charge transfer resistance decreased. This finding was completely in agreement with the results of the LSV test and revealed that the current density of 500 mA/cm<sup>2</sup> had the lowest charge transfer resistance for HER while exhibiting the highest electrocatalytic properties. Table 2 shows the values of the parameters obtained from the equivalent circuit of the EIS test. As can be seen,

the current density of 500 mA/cm<sup>2</sup> has the lowest resistance. Moreover, Y<sub>0</sub>-CPE is the highest value in this coating, which indicates the highest number of active sites on the coating surface. These active sites play an important role in electron transfer between the coating and hydrogen.



**Fig. 4.** Nyquist diagrams obtained from the EIS test on Ni-W coating electrodeposited with different current densities.

### 3.2.3. Chronoamperometry results

Steadiness and performance stability during the service life are of great importance for industrial catalysts. To investigate this factor, chronoamperometry was performed at a negative cathodic constant potential of 1.5 V with respect to the calomel reference electrode. The results presented in Fig. 5 prove the appropriate stability of the samples. It was also found that at the same potential, the coating applied at a higher current density showed a higher current density of hydrogen evolution and therefore had better performance.

### 3.2.4. Cyclic voltammetry results

To evaluate the active surface area of the electrodes, the cyclic voltammetry test was carried out at different scanning rates and the results are shown in Fig. 6. In this test, the active surface area of the electrodes is directly related to C<sub>dl</sub> and increasing the slope of the current density graph in terms of the scanning rate indicates a rise in the surface area of the

coating which is determined using the equation (1) :  

$$|\Delta i| = 2 (C_{dl} \times v) \quad (1)$$
 where  $v$  is the potential sweep rate, and  $|i|$  is the charging current density. As illustrated in Fig. 6, when the plating current density increases, C<sub>dl</sub> has increased from 248 to 1310 μF/cm<sup>2</sup> and the active surface area significantly grows as well.

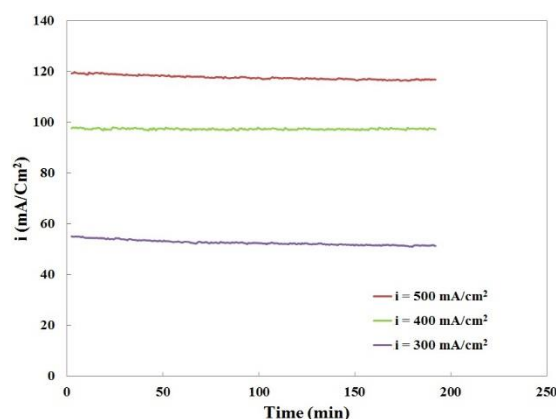


**Fig. 5.** Results of chronoamperometry of Ni-W coating electrodeposited with different current densities.

## 4. CONCLUSIONS

In summary, Nickel-tungsten coating was synthesized in different current densities on the low-carbon steel substrate and the following results were obtained.

- 1) By increasing the current density of electrodeposition up to 500 mA/cm<sup>2</sup>, Ni-W coatings with high porosity, columnar morphology, and high active surface were obtained.
- 2) The cyclic voltammetry test (CV) revealed that when the plating current density increases, C<sub>dl</sub> increases from 248 to 1310 μF/cm<sup>2</sup> and the active surface area increases 5 times.
- 3) Moreover, by expanding the active surface of the coating, at a certain overpotential, the amount of cathodic current density increased, which indicates enhanced electrocatalytic property and HER.
- 4) This method is an efficient and facile approach to improving the electrocatalytic properties of the coating.

**Table 2.** Values of parameters of the equivalent circuit of the EIS test performed on Ni-W coating electrodeposited at different current densities.

$i$ (mA.cm <sup>-2</sup> )	$R_s$ (Ω.cm <sup>2</sup> )	$R_p$ (Ω.cm <sup>2</sup> )	$Y_0$ - CPE (Ω <sup>-2</sup> .cm <sup>-2</sup> .s <sup>n</sup> )	$n$
500	9.08	36	11.3	0.62
400	8.91	59	7.1	0.68
300	9.13	136	0.9	0.75



**Fig. 6.** Results of cyclic voltammetry test of Ni-W coating electrodeposited with different current densities, a) 500, b) 400, c) 300 mA/cm<sup>2</sup>.

## REFERENCES

- [1]. Mahmoud KG, Abualreish MJA, Khairy M., "Nanosized nickel hexacyanoferrate modified platinum electrode for promoting hydrogen evolution reaction in alkaline medium." *Journal of Electroanalytical Chemistry*. 2023, 940, 117513.
- [2]. Wang H, Xie M, Zong Q, Liu Z, Huang X, Jin Y., "Electroless Ni-W-Cr-P alloy coating with improved electrocatalytic hydrogen evolution performance." *Surface Engineering*. 2015, 31(3), 226-31.
- [3]. Khajehsaeidi Z, Sangpour P, Ghaffarinejad

- A., "A novel co-electrodeposited Co/MoSe<sub>2</sub>/reduced graphene oxide nanocomposite as electrocatalyst for hydrogen evolution." *International Journal of Hydrogen Energy*. 2019, 44(36), 19816-26.
- [4]. Uzal H, Döner A, Bayrakçeken H., "Preparation and fabrication of NiCo coated TiO<sub>2</sub>-NTs for hydrogen evolution." *Energy Sources, Part A: Recovery, Utilization, and Environmental Effects*. 2022, 44(2), 3406-17.
- [5]. Vincent I, Bessarabov D., "Low cost hydrogen production by anion exchange membrane electrolysis: A review." *Renewable and Sustainable Energy Reviews*. 2018, 81, 1690-704.
- [6]. Vernickaite E, Tsyntaru N, Sobczak K, Cesiulis H., "Electrodeposited tungsten-rich Ni-W, Co-W and Fe-W cathodes for efficient hydrogen evolution in alkaline medium." *Electrochimica Acta*. 2019, 318, 597-606.
- [7]. Cheng Y., "Advances in electrocatalysts for oxygen evolution reaction of water electrolysis-from metal oxides to carbon nanotubes." *Progress in natural science: materials international*. 2015, 25(6), 545-53.
- [8]. Zhang X, Fan Y, Zhang W, Tang L, Guo J., "Coupled Co and Ir nanocrystals on graphite as pH-wide and efficient electrocatalyst for hydrogen evolution. *Surfaces and Interfaces*." 2021, 24, 101049.
- [9]. Zhang Q, Chen D, Song Q, Zhou C, Li D, Tian D, "Holey defected TiO<sub>2</sub> nanosheets with oxygen vacancies for efficient photocatalytic hydrogen production from water splitting." *Surfaces and Interfaces*. 2021, 23, 100979.
- [10]. Xu X, Zhong W, Zhang L, Liu G, Xu W, Zhang Y, "NiCo-LDHs derived NiCo<sub>2</sub>S<sub>4</sub> nanostructure coated by MoS<sub>2</sub> nanosheets as high-efficiency bifunctional electrocatalysts for overall water splitting." *Surface and Coatings Technology*. 2020, 397, 126065.
- [11]. Bélanger A, Vijh AK., "The hydrogen evolution reaction on Ni-Sn alloys and intermetallics." *Surface and Coatings Technology*. 1986, 28(1), 93-111.
- [12]. Zheng Y, Jiao Y, Zhu Y, Li LH, Han Y, Chen Y., "Hydrogen evolution by a metal-free electrocatalyst." *Nature communications*. 2014, 5(1), 1-8.
- [13]. Conway B, Tilak B., "Interfacial processes involving electrocatalytic evolution and oxidation of H<sub>2</sub>, and the role of chemisorbed H." *Electrochimica Acta*. 2002, 47(22-23), 3571-94.
- [14]. Vrabel H, Merki D, Hu X., "Hydrogen evolution catalyzed by MoS<sub>3</sub> and MoS<sub>2</sub> particles." *Energy & Environmental Science*. 2012, 5(3), 6136-44.
- [15]. Gao G, Wang W, Wang Y, Fu Z, Liu L, Du Y, et al., "Synergistic coupling of NiCoS nanorods with NiCo-LDH nanosheets towards highly efficient hydrogen evolution reaction in alkaline media." *Journal of Electroanalytical Chemistry*. 2023, 117622.
- [16]. Loiacono A, Diaz-Coello S, Garcia G, Lacconi GI, Rodriguez JL, Pastor E, et al., "Nickel-based composites using tungsten carbides as enhancers for electroactivity for the hydrogen evolution reaction." *Journal of Electroanalytical Chemistry*. 2023, 117973.
- [17]. Feng Y, Wei Y, Liu S, Li P, Akhtar K, Bakhsh EM, et al., "Enhanced hydrogen evolution reaction activity of FeNi layered double hydroxide modified with Ruthenium nanoparticles at high current density." *Journal of Electroanalytical Chemistry*. 2023, 938, 117451.
- [18]. Moein A, Rastegari S., "Effect of pulse parameters on the morphology of electroplated Ni-W-TiC nanocomposite coating." *Surface Engineering*. 2020, 36(9), 982-9.
- [19]. Goldasteh H, Rastegari S., "The influence of pulse plating parameters on structure and properties of Ni-W-TiO<sub>2</sub> nanocomposite coatings." *Surface and Coatings Technology*. 2014, 259, 393-400.
- [20]. Loiacono A, Gutiérrez-Tarriño S, Llorente VB, Lacconi G, Oña-Burgos P, Franceschini EA., "Ni/Ru@ NC-CeO<sub>2</sub> composite for hydrogen evolution reaction in alkaline media: Effect of CeO<sub>2</sub> decoration with Ru@ NC on the catalytic activity." *Journal of Electroanalytical Chemistry*. 2023, 941, 117548.



- [21]. Allam M, Benaicha M, Dakhouche A., "Electrodeposition and characterization of NiMoW alloy as electrode material for hydrogen evolution in alkaline water electrolysis." *International Journal of Hydrogen Energy*. 2018, 43(6), 3394-405.
- [22]. Minaev P, Nikulshin P, Kulikova M, Pimerzin A, Kogan V., "NiWS/Al<sub>2</sub>O<sub>3</sub> hydrotreating catalysts prepared with 12-tungstophosphoric heteropolyacid and nickel citrate: Effect of Ni/W ratio." *Applied Catalysis A: General*. 2015, 505, 456-66.
- [23]. Hong SH, Ahn SH, Choi J, Kim JY, Kim HY, Kim H-J, et al., "High-activity electrodeposited NiW catalysts for hydrogen evolution in alkaline water electrolysis. *Applied Surface Science*." 2015, 349, 629-35.
- [24]. Metikoš-Huković M, Grubač Z, Radić N, Tonejc A., "Sputter deposited nanocrystalline Ni and Ni-W films as catalysts for hydrogen evolution. *Journal of Molecular Catalysis A: Chemical*." 2006, 249(1-2), 172-80.
- [25]. Rad PJ, Aliofkhazraei M, Darband GB., "Ni-W nanostructure well-marked by Ni selective etching for enhanced hydrogen evolution reaction." *International Journal of Hydrogen Energy*. 2019, 44(2), 880-94.
- [26]. Ahn SH, Choi I, Park H-Y, Hwang SJ, Yoo SJ, Cho E, et al., "Effect of morphology of electrodeposited Ni catalysts on the behavior of bubbles generated during the oxygen evolution reaction in alkaline water electrolysis." *Chemical communications*. 2013, 49(81), 9323-5.
- [27]. Elias L, Scott K, Hegde AC., "Electrolytic synthesis and characterization of electrocatalytic Ni-W alloy." *Journal of Materials Engineering and Performance*. 2015, 24(11), 4182-91.
- [28]. Badawy W, Feky H, Helal N, Mohammed H., "Cathodic hydrogen evolution on molybdenum in NaOH solutions." *International journal of hydrogen energy*. 2013, 38(23), 9625-32.